Check for updates

N-Iodophthalimide as a halogen bond donor, a comparison with *N*-iodosuccinimide and *N*-iodosaccharin†

Ie-Rang Jeon, [iD] Olivier Jeannin, [iD] Antoine Robert, Frédéric Barrière and Marc Fourmigué [iD] *

We investigate here the ability of *N*-iodophthalimide (NIPht) to act as a halogen bond (HaB) donor, in comparison with well-known HaB donors *N*-iodosuccinimide (NISucc) and *N*-iodosaccharin (NISacc). The structure of NIPht itself is reported, together with those of neutral adducts with 4-dimethylaminopyridine (DMAP), 4,4′-bipyridine and 2,2′-bipyridine derivatives. Comparison with analogous adducts involving NISucc and NISacc shows that NIPht behaves essentially like NISucc as a HaB donor, both forming weaker adducts than NISacc with a given Lewis base. A symmetric anionic complex [NPht–I–NPht]⁻ is isolated in the presence of [K(18-crown-6)]⁺. It exhibits N–I distances very close to those observed in the known [NSucc–I–NSucc]⁻ and [NSacc–I–NSacc]⁻ species (2.24–2.26 Å), confirming the 3-center–4-electron (3c–4e) character of the bonding in these species. This similarity confirms the peculiar character of the only other reported salt of [NPht–I–NPht]⁻, namely [Me₄N][NPht–I–NPht], where the longer N–I distances (2.29 Å) are a consequence of a specific solid-state arrangement and C–H···O hydrogen bonds.

Introduction

Because of its strength and directionality, halogen bonding (HaB) is currently considered as the prototypical σ-hole interaction, where the halogen atom acts as the electrophile.[1] This interaction plays a crucial role in many areas of supramolecular chemistry and crystal engineering and has been shown to be the strongest in the halogen series in the order I > Br ≫ Cl ≫ F.[2] Covalently linked iodine atoms are more prone to exhibit such strong σ-holes when properly activated by electron-withdrawing groups, as in perfluoroalkyl, perfluoroaryl or alkynyl iodide derivatives. When iodine is covalently linked to a nitrogen atom, strong σ-holes can also be found, for example in cationic *N*-iodopyridinium species, providing the symmetric [Py–I–Py]⁺ cation.[3,4] Neutral halogen-bonded adducts are found with *N*-iodoimides (Fig. 1a) such as *N*-iodosuccinimide (NISucc)[5,6] or *N*,*N*′-diiodohydantoins (DIH),[7] or with *N*-iodosulfamides such as *N*-iodosaccharin (NISacc) as HaB donors.[8] Each of them gives rise to many reported examples of halogen-bonded adducts, essentially

with pyridines[9,10] and pyridine *N*-oxides.[11] Symmetric (or close-to-symmetric) anionic systems were also described upon the interaction of a HaB donor such as, for example, NISacc with the corresponding saccharinate anion to give the symmetric [NSacc–I–NSacc]⁻ anion (Fig. 1a).[12,13]
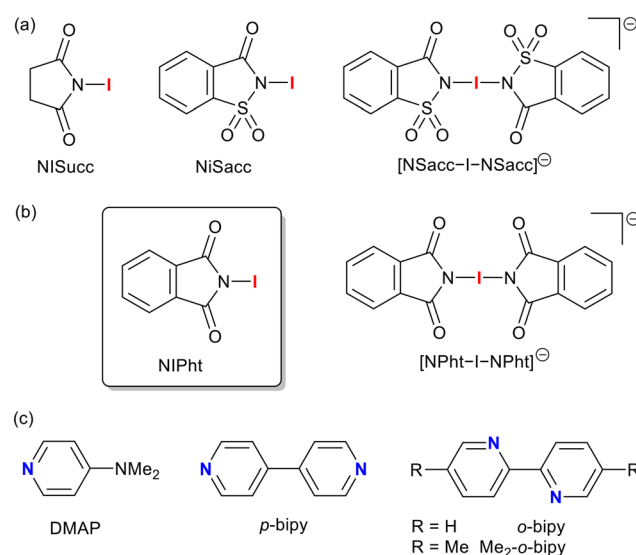

Fig. 1 Chemical structures of (a and b) the investigated HaB donors NISucc, NISacc and NIPht and their anionic complexes and (c) the investigated HaB acceptors.

UnivRennes, CNRS, ISCR (Institut des Sciences Chimiques de Rennes), Campus de Beaulieu, Rennes, 35000, France. E-mail: marc.fourmigue@univ-rennes.fr

Surprisingly, among the different *N*-iodoimides, *N*-iodophthalimide (NIPht, Fig. 1b), a well-known iodinating agent in organic chemistry,[14] has not been reported to act as an HaB donor in the solid state, perhaps because it is not commercially available. Only one acetonitrile adduct of the perfluoro-*N*-iodophthalimide has been reported to date,[15] while, very recently, the crystal structure of the symmetric anion [NPht–I–NPht]⁻ was described as a Me₄N⁺ salt and characterized by a short N–I bond (2.293(11) Å) and a linear geometry (N–I–N angle at 180°).[13] Although these structural characteristics are very close to those reported for other HaB donors such as NISucc and NISacc in similar symmetric [NSucc–I–NSucc]⁻ and [NSacc–I–NSacc]⁻ anions,[12,13] they do not allow, in a first approximation, for a ranking of the HaB donor strength between these different HaB donors.

In order to evaluate the ability of NIPht to enter in such halogen-bonded cocrystals, we have investigated their formation with different pyridines as Lewis bases, and we were able to crystallize and structurally characterize three different halogen-bonded adducts of NIPht with, respectively, 4-dimethylaminopyridine (DMAP), 4,4′-bipyridine and 2,2′-bipyridine (Fig. 1c), allowing thus for useful comparisons of the structural characteristics of the adducts with those obtained with NISacc or NISucc and the same pyridine-based HaB acceptors. Besides, we were also able to isolate and structurally characterize a second example of the symmetric anionic [NPht–I–NPht]⁻ species as its [(18-crown-6)K⁺] salt, at variance with the only reported Me₄N⁺ salt.[13] The evolution of the N–I distances within the [NPht–I–NPht]⁻ species as a function of the nature of the cation counterbalancing its charge will also be analyzed.

Results and discussion

NIPht was prepared, as previously described, from phthalimide, PhI(OAc)₂ and I₂ in 99% yield.[16] It crystallizes in the orthorhombic system, space group $P2_12_12_1$ with one molecule in the general position in the unit cell. As shown in Fig. 2, the molecules are associated into chains running along *b* through the 2_1 screw axis, with a short and linear
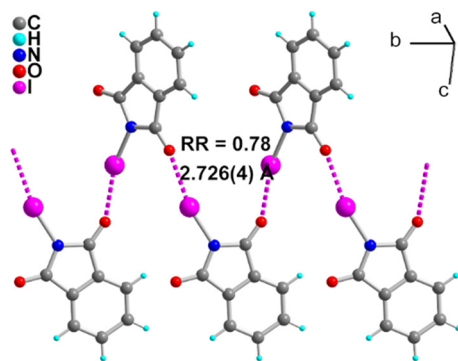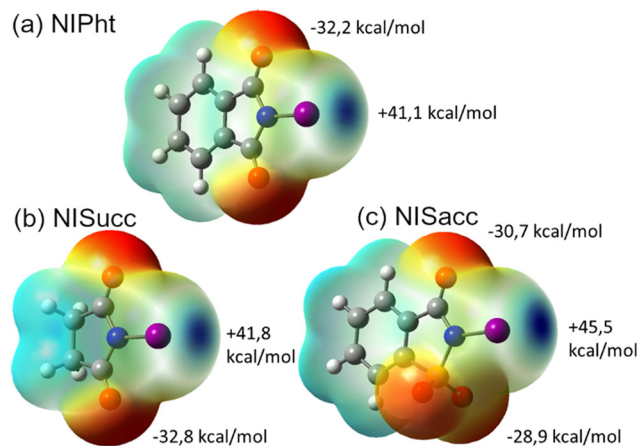

Fig. 3 Molecular electrostatic potential surface at an isovalue of 0.001 for (a) NIPht, (b) NISucc and (c) NISacc (B3LYP/6-31G**-LANLdp, Gaussian16 Rev A.03) with extrema values at oxygen and iodine atoms indicated. Red indicates a negative charge density and blue, a positive charge density. The full-scale range is −0.0522/+0.0725 au (Hartrees), *i.e.* −32.8/+45.5 kcal mol⁻¹ for the three compounds.

HaB with an I⋯O distance at 2.726(4) Å (RR = 0.78), N–I⋯O angle at 166.8(1)° and C=O⋯I angle at 146.4(3)°. These values can be compared with those reported in the structure of NISucc,[5] [I⋯O: 2.580(6) Å (RR = 0.74), N–I⋯O: 175.7(2)°, and C=O⋯I: 121.6°(5)], indicating that NIPht appears as a slightly weaker HaB donor than NISucc, with, nevertheless a good HaB ability characterized with this RR = 0.78 value for the N–I⋯O=C interaction. This is also confirmed by the evolution on the covalent N–I bond length, observed here at 2.034(4) Å, while it is found slightly more elongated in NISucc at 2.060(6) Å, another signature of a stronger HaB interaction in NISucc. Note that a similar comparison with the structure of NISacc itself cannot be conducted as its structure is reported as a solvate with one water molecule acting as the HaB acceptor, rather than a carbonyl or sulfonyl oxygen atom.[8]

Calculations of the ESP extremum of the σ-hole on each of these three HaB donors, namely, NIPht, NISucc and NISacc were conducted to possibly propose a ranking of the three HaB donors. Indeed, since halogen bonding is primarily electrostatic in nature,[17,18] a measure of the halogen bond donor character can be given by the maximum value of the molecular surface electrostatic potential at the iodine atom ($V_{S,max}$). As shown in Fig. 3, it appears that NIPht exhibits the smallest calculated $V_{s,max}$ value (+41.1 kcal mol⁻¹) of the three HaB donor molecules. Nevertheless, this $V_{s,max}$ value is very
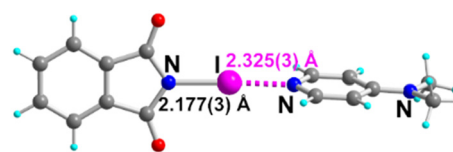

Fig. 2 Details of the HaB interaction (as pink dotted lines) in the structure of NIPht.

Fig. 4 Molecular structure of the NIPht·DMAP adduct. The HaB interaction is depicted as a pink dotted line.

Table 1 Structural characteristics of the HaB interactions in the DMAP adducts of NIPht, NISucc and NISacc (distances in Å and angles in °)

	$T(\text{K})$	N–I dist.	I···N_{DMAP} dist.	N–I···N_{DMAP} angle	N···N_{DMAP} dist.	Ref.
NISucc·DMAP	RT	2.146(4)	2.407(4)	178.9(1)	4.553(6)	9a
	RT	2.138(5)	2.403(6)	178.7(2)	4.541(8)	6
NIPht·DMAP	150(2)	2.177(3)	2.325(3)	177.68(5)	4.501(6)	This work
NISacc·DMAP	150(2)	2.292(2)	2.218(2)	178.5(1)	4.509(3)	9a
	RT	2.292(1)	2.228(1)	178.8(1)	4.520(1)	9a

close to that found for NISucc (+41.8 kcal mol⁻¹) and exceeds those calculated under the same conditions for well-known HaB donors such as C_6F_5–I (+35.1 kcal mol⁻¹) or Ph–C≡C–I (+34.6 kcal mol⁻¹) (Fig. S1†), indicating that NIPht should definitely act as a good HaB donor.

Cocrystal structures within neutral adducts

Co-crystallization experiments of NIPht were accordingly conducted with 4-dimethylaminopyridine (DMAP), 4,4′-bipyridine, 2,2′-bipyridine, and its substituted analog 5,5′-dimethyl-2,2′-bipyridine, abbreviated, respectively, as *p*-bipy, *o*-bipy and Me₂-*o*-bipy (Fig. 1c). The use of these geometrically constrained *o*-bipy or Me₂-*o*-bipy molecules, furthermore blessed with a decreased Lewis base character compared with *p*-bipy, was indeed considered to test the evolution of the HaB strength. Crystals amenable to X-ray diffraction were obtained with the four pyridine derivatives, with the following composition, NIPht·DMAP, (NIPht)₂·(*p*-bipy), (NIPht)₂·(*o*-bipy) and (NIPht)₂·(Me₂-*o*-bipy).

Fig. 5 Details of the α-(NIPht)₂(*p*-bipy) adduct, viewed (a) perpendicular to the *p*-bipy plane and (b) parallel to the *p*-bipy plane, and of the β-(NIPht)₂(*p*-bipy) adduct, viewed (c) perpendicular to the *p*-bipy plane and (d) parallel to the *p*-bipy plane. The HaB interaction is depicted as pink dotted lines.

NIPht·DMAP crystallizes in the monoclinic system, space group $P2_1/n$. As shown in Fig. 4, the iodine atom is engaged in a short and linear HaB interaction with the pyridinic nitrogen atom. Note also that the molecular planes of both partners are almost perpendicular to each other, with a plane-to-plane angle of 85.7(4)°. Structural characteristics of the HaB interaction are collected in Table 1, together with the reported data for similar DMAP adducts of NISacc and NISucc. We note here that, despite a slightly weaker σ-hole on iodine, the HaB interaction with NIPht is stronger than that with NISucc, with a shortening of the I···N_{DMAP} HaB length and a concomitant lengthening of the "covalent" N–I bond length.

Cocrystallization of NIPht with 4,4′-bipyridine (*p*-bipy) afforded two different phases (see the ESI†). Both adopt a 2 : 1 stoichiometry, α-(NIPht)₂(*p*-bipy) in the monoclinic P2₁/n space group and β-(NIPht)₂(*p*-bipy) in the monoclinic $P2_1/c$ space group, with, in both structures, the adduct located on an inversion center (Fig. 5). As shown in Table 2, characteristic N–I and I···N_{bipy} bond distances are, within a 3σ tolerance, the same in both phases. The main difference is found in the plane-to-plane angle between the NIPht and *o*-bipy moieties, at θ = 20.4(2)° in α-(NIPht)₂(*p*-bipy) (Fig. 5b) but at θ = 52.5(1)° in β-(NIPht)₂(*p*-bipy) (Fig. 5d). This difference brings important consequences on the solid-state association of the adducts in the crystal, with a face-to-face stacking of the close-to-planar adducts in the α-phase, but a more complex organization in the β-phase (Fig. S2†).

In order to allow for a comparison of NIPht with the other HaB donors, NISucc and NISacc, we also attempted the preparation of their respective adducts with 4,4′-bipyridine. Our trials were unsuccessful with NISucc, but crystals of good quality could be obtained with NISacc. (NISacc)₂(*p*-bipy) adopts a very similar geometry (Fig. 6), with notably stronger HaB interactions than those with NIPht (Table 2), and with a plane-to-plane angle between NISacc and the pyridine moieties of θ = 56.8(2)° (Fig. 6b).

Cocrystals with the sterically demanding 2,2′-bipyridine were also investigated but our efforts to isolate good quality cocrystals with NIPht for satisfactory refinements were unsuccessful (unit cell parameters are reported in the ESI†). We therefore also considered the dimethyl analog, 5,5′-dimethyl-2,2′-bipyridine (*o*-Me₂bipy) and were able to isolate good quality crystals of the 2 : 1 adduct with NIPht as a CH₂-Cl₂ solvate, formulated as (NIPht)₂(*o*-Me₂bipy)·(CH₂Cl₂). It crystallizes in the orthorhombic system, space group *Pba*2, with the adduct located on a 2-fold axis (Fig. 7). The
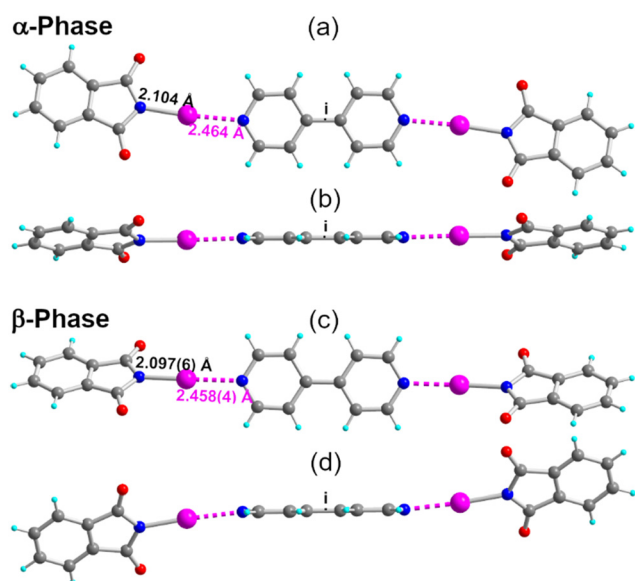
Table 2 Structural characteristics of the HaB interactions in the *p*-bipy adducts of NIPht and NISacc (distances in Å and angles in °). θ is defined as the angle between the molecular planes of the HaB donor and the pyridinic ring

	T(K)	N–I dist.	I⋯N_{Py} dist.	N–I⋯N_{Py} angle	N⋯N_{Py} dist.	θ angle
(NIPht)$_2$(*p*-bipy): α-phase	296(2)	2.104(5)	2.464(5)	176.2(2)	4.565(7)	20.4(2)
β-phase	296(2)	2.097(6)	2.458(4)	176.79(16)	4.553(7)	52.5(1)
(NISacc)$_2$(*p*-bipy)	296(2)	2.173(6)	2.346(6)	176.4(2)	4.517(8)	56.8(2)

o-Me$_2$bipy molecule itself is not planar with a N_{bipy}–C–C–N_{bipy} torsion angle ψ that amounts to +143.0(7)° (Table 3). Also, as already observed in the *para* analog (NIPht)$_2$(*p*-bipy), the NIPht moiety is not coplanar with the pyridinyl ring but makes an angle θ of 28°. The HaB interaction with the I⋯N_{Py} distance at 2.624(4) Å is also notably weaker than that with the *para* analogs α/β-(NIPht)$_2$(*p*-bipy), where it is found at ≈2.46 Å.

To further strengthen our comparison with the two other HaB donors NISucc and NISacc, we also investigated their adducts with *o*-bipy and Me$_2$-*o*-bipy and were able to isolate and structurally characterize three of them, namely, (NISucc)$_2$(*o*-bipy), (NISucc)$_2$(*o*-Me$_2$bipy) and (NISacc)$_2$(*o*-bipy). As shown in Fig. 8 and Table 3, they adopt different geometries, particularly with respect to the $N_{py}CCN_{py}$ torsion angle ψ between the two pyridine rings, adopting an anticlinal conformation with three of them while the (NISucc)$_2$(*o*-Me$_2$bipy) exhibits a synclinal conformation with $30° < \psi < 90°$. All adducts with NISucc and NISacc exhibit a stronger HaB interaction than that with NIPht, with the I⋯N Py distance in the 2.44–2.52 Å range, to be compared with the 2.624(6) Å value found with NIPht in (NIPht)$_2$(*o*-Me$_2$bipy).

In conclusion of this part dedicated to neutral halogen-bonded adducts, the evolution of the HaB strength of NIPht *vs.* the different Lewis bases explored here, namely, DMAP, *p*-bipy and *o*-Me$_2$bipy follows the trends observed with other HaB donors, with a ranking DMAP > *p*-bipy > *o*-Me$_2$bipy. Indeed, the overall decreased Lewis base character of 2,2′-bipyridines was discussed by Pennington *et al.*[19] in cocrystals of *p*-diiodotetrafluorobenzene with *p*-bipy,[20] *o*-bipy,[21] and Me$_2$-*o*-bipy.[19] This ranking is also in line with the diiodine basicity scale defined by Laurence *et al.*[22] who determined

the pK_{BI2} values of 3.78 for DMAP, 2.22 for pyridine itself, 1.81 for *p*-bipy and 0.62 for *o*-bipy.

The different systems described above, in neutral adducts with pyridine-based Lewis bases, allow us to establish the HaB donor ability of NIPht, by comparison with other well-known HaB donors such as NISucc and NISacc. With such neutral pyridines, it appears that NIPht is always a weaker HaB donor than NISacc, as anticipated from the large difference of the calculated extrema of the electrostatic potential on iodine (Fig. 3). The comparison with NISucc is ambiguous, as NIPht appears to give a notably stronger HaB than NISucc with DMAP, but a weaker one with the other Lewis bases (*o*-bipy and *o*-Me$_2$bipy) investigated here. Altogether both HaB donors NIPht and NISucc behave very closely.

The anionic [NPht–I–NPht]⁻ species

As mentioned in the Introduction, symmetric (or close-to-symmetric) anionic systems involving NIPht (and other *N*-iodiimides) were already described upon interactions of an HaB donor such as NIPht with the corresponding phthalimidate anion to give the symmetric [NPht–I–NPht]⁻ anion (Fig. 1b). In such systems, the covalent part of the N–I bond is enhanced up to the point that they have been described as 3-center–4-electron bonds. Several examples were reported with the bromine analog [NPht–Br–NPht]⁻ while the iodine derivatives are known with NISucc in [Bu$_4$N][NSucc–I–NSucc][23] and with NISacc in [Bu$_4$N][NSacc–I–NSacc].[12,13] One single example has been reported to date involving NIPht, namely, the tetramethylammonium salt [Me$_4$N][NPht–I–NPht].[13] We report here another example of this [NPht–I–NPht]⁻ anion prepared directly from NIPht and potassium phthalimidate in the presence of 18-crown-6, allowing the isolation of [K(18-crown-6)][NPht–I–NPht]. It
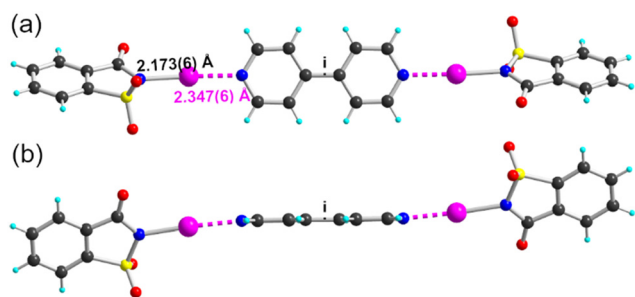
Fig. 6 Molecular structure of the (NISacc)$_2$(*p*-bipy) adduct, viewed (a) perpendicular to the *p*-bipy plane and (b) parallel to the *p*-bipy plane. The HaB interaction is depicted as pink dotted lines.
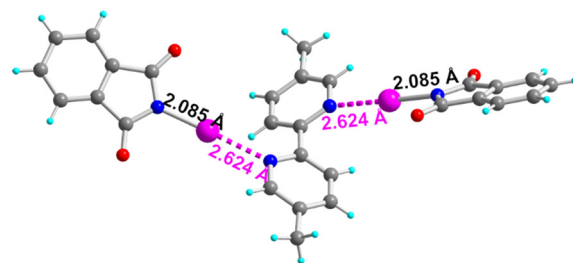
Fig. 7 Details of the solid-state association in the (NIPht)$_2$(*o*-Me$_2$bipy) adduct.

Table 3 Structural characteristics of the HaB interactions in the *o*-bipy and *o*-Me$_2$bipy adducts of NIPht, NISucc and NISacc (distances in Å and angles in °). θ is defined as the angle between the molecular planes of the HaB donor and the pyridinic ring

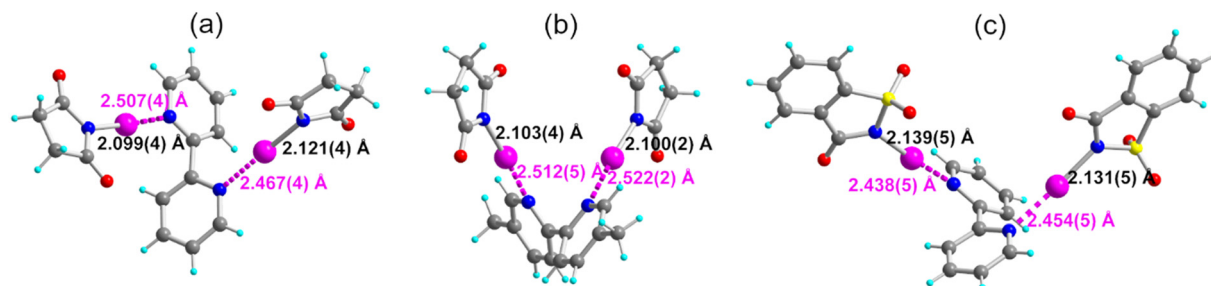|	T(K)	N–I dist.	I···N$_{Py}$ dist.	N–I···N$_{Py}$ angle	N···N$_{Py}$ dist.	ψ N$_{Py}$CCN$_{Py}$ torsion angle	θ angle
(NIPht)$_2$(*o*-Me$_2$bipy)	296(2)	2.085(6)	2.624(6)	178.9(2)	4.709(9)	+143.0(7)	28(1)
(NISucc)$_2$(*o*-bipy)	150(2)	2.121(4)	2.467(4)	177.26(7)	4.587(7)	−117.3(2)	84(1)
		2.099(4)	2.507(4)	176.53(7)	4.604(7)		11(1)
(NISucc)$_2$(*o*-Me$_2$bipy)	150(2)	2.103(4)	2.512(5)	175.09(6)	4.611(8)	+56.4(22)	58.5(5)
		2.100(2)	2.522(2)	175.41(6)	4.619(4)		60.0(1)
(NISacc)$_2$(*o*-bipy)	296(2)	2.139(5)	2.438(5)	175.4(1)	4.573(7)	−132.7(4)	80.0(1)
		2.131(5)	2.454(5)	174.2(1)	4.580(9)		79.7(1)

Fig. 8 Molecular structure of the three adducts with 2,2′-bipyridines: (a) (NISucc)$_2$(*o*-bipy), (b) (NISucc)$_2$(*o*-Me$_2$bipy) and (c) (NISacc)$_2$(*o*-bipy). The HaB interaction is depicted as pink dotted lines.

crystallizes in the triclinic system, space group $P\bar{1}$ with both ions in the general position (Fig. 9). We have reported in Table 4 the structural characteristics of the anion, together with those reported for [Me$_4$N][NPht–I–NPht], as well as the Bu$_4$N$^+$ salts of the analogous NISucc and NISacc derivatives.

As shown in Fig. 9, the potassium cation completes its coordination sphere with two carbonyl oxygen atoms of the phthalimidate moieties in apical positions, leading to the formation of supramolecular chains with an alternation of cationic and anionic moieties. The two K$^+$···O contact lengths are comparable, as well as the two N–I bond lengths in the [NPht–I–NPht]$^-$ anion (Table 4), giving an essentially symmetric complex (at the 3σ level).

By analogy with other reports on analogous structures with NISacc (see below), the angle between the two

Fig. 9 Details of the solid-state association within [K(18-crown-6)] [NPht–I–NPht] showing the chain-like motif formed by coordination with the [K(18-crown-6)]$^+$ cation.

phthalimidate molecular planes is illustrated here by the C–N···N–C dihedral angle, here at 7.7(4)°, indicating a close-to-planar conformation. The N–I distances compare very well with those reported in other systems with NISucc and NISacc and appear therefore to be somehow independent of the nature of the imidato anions surrounding the iodonium moiety, an observation in line with the strong covalency of the N–I bonds in these 3-center–4-electron (3c–4e) systems. In that respect, the reported tetramethyammonium salt of [NPht–I–NPht]$^-$ appears as unusual, with notably longer N–I bonds (Table 4). This was attributed to the presence of hydrogen bonds with the Me$_4$N$^+$ cation, which leads to the formation of ···[Me$_4$N]$^+$··· [NPht–I–NPht]$^-$···[Me$_4$N]$^+$···[NPht–I–NPht]$^-$··· chains (Fig. S3†). However, a closer inspection of the two other reported systems with NISucc and NISacc as Bu$_4$N$^+$ salts also reveals the presence of similar (or even shorter) hydrogen bonds involving the hydrogen atoms of the α-methylene moieties in Bu$_4$N$^+$ (Fig. S4 and Table S3†). We believe that besides these HBs, it is also the rigidity of the Me$_4$N$^+$ cation that pushes away the two phthalimidate from the iodonium cation in [Me$_4$N][NPh–I–NPht], while such an effect is absent in the Bu$_4$N$^+$ salts of [NSucc–I–NSucc]$^-$ and [NSacc–I–NSacc]$^-$ and in the [K(18-crown-6)]$^+$ salt reported here, which all exhibit N–I distances in the same range.

Conclusions

We have demonstrated here with several examples that NIPht, like the well-known NISucc and NISacc compounds, can act as a powerful HaB donor through its σ-hole on
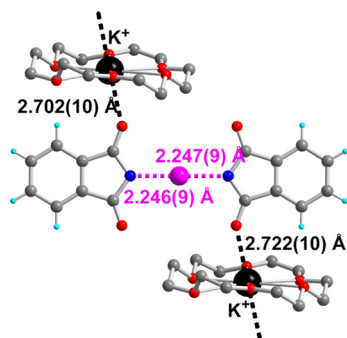
Table 4 Structural characteristics of the HaB interactions in [K(18-crown-6)][NPht–I–NPht] and reference salts (distances in Å and angles in °)

	T(K)	N–I dist.	I–N dist.	N–I–N angle	N⋯N dist.	CN⋯NC torsion angle	Ref.
[NPht–I–NPht]⁻[a]	296(2)	2.246(9)	2.247(9)	179.7(1)	4.493(18)	7.7(4)[d]	This work
[NPht–I–NPht]⁻[b]	170(2)	2.293(11)	2.293(11)	180.00	4.587(16)	0.5(4)[d]	13
[NSucc–I–NSucc]⁻[c]	100	2.264(2)	2.244(2)	179.57(6)	4.508(2)	36.7(2)[d]	23
[NSacc–I–NSacc]⁻[c]	100	2.247(5)	2.250(5)	176.82(12)	4.495(8)	36.2(4)	12

[a] As the [K(18-crown-6)]⁺ salt. [b] As the Me₄N⁺ salt. [c] As the Bu₄N⁺ salt. [d] The lowest of the possible C–N⋯N–C torsion angles is reported.

iodine, whose amplitude is comparable to that of NISucc but notably smaller than that of NISacc. HaB interactions within neutral adducts with pyridines compare with those found with NISucc, allowing for a NIPht ≈ NISucc < NISacc ranking. A second example of the negatively charged, essentially symmetric [NPht–I–NPht]⁻ species is isolated here as the [K(18-crown-6)]⁺ salt, with N–I distances comparable to those observed in other 3c–4e systems such as [NSucc–I–NSucc]⁻ and [NSacc–I–Sacc]⁻. The carbonyl oxygen atoms of the phthalimidate moieties are involved in the coordination sphere of the [K(18-crown-6)]⁺ cation, allowing for the formation of a 1-D polymer in the solid state.

Experimental

All experimental information (synthesis, characterization data, crystal growth conditions, X-ray crystallography and DFT calculations of ESP maps) are in the ESI.†

Data availability

The data supporting this article have been included as part of the ESI.†

Crystallographic data have been deposited at the CCDC under CCDC numbers 2366101–2366110 for, respectively, compounds NIPht, (NIPht)·DMAP, α-(NIPht)₂(p-bipy), β-(NIPht)₂(*p*-bipy), (NIPht)₂(*o*-Me₂bipy)·CH₂Cl₂, (NISacc)₂(*p*-bipy), (NISucc)₂(*o*-bipy), (NISucc)₂(*o*-Me₂bipy), (NISacc)₂(*o*-bipy) and [K(18-crown-6)][NPht–I–NPht] and can be obtained directly from **https://www.ccdc.cam.ac.uk/products/csd/request/request.php4**.

Author contributions

I.-R. J. and M. F. formulated the project. A. R. and I.-R. J. synthesized and crystallized the compounds. O. J. collected and solved X-ray diffraction data. F. B. performed the DFT calculations. M. F. wrote the paper and all the authors contributed to revising it.

Conflicts of interest

There are no conflicts to declare.

Acknowledgements

References

1 G. R. Desiraju, P. S. Ho, L. Kloo, A. C. Legon, R. Marquardt, P. Metrangolo, P. Politzer, G. Resnati and K. Rissanen, *Pure Appl. Chem.*, 2013, **85**, 1711–1713.

2 (*a*) G. Cavallo, P. Metrangolo, R. Milani, T. Pilati, A. Priimagi, G. Resnati and G. Terraneo, *Chem. Rev.*, 2016, **116**, 2478–2601; (*b*) L. C. Gilday, S. W. Robinson, T. A. Barendt, M. J. Langton, B. R. Mullaney and P. D. Beer, *Chem. Rev.*, 2015, **115**, 7118–7195; (*c*) M. H. Kolár and P. Hobza, *Chem. Rev.*, 2016, **116**, 5155–5187; (*d*) H. Wang, W. Wang and W. J. Jin, *Chem. Rev.*, 2016, **116**, 5072–5104.

3 (*a*) J. A. Creighton, I. Haque and J. L. Wood, *Chem. Commun.*, 1966, 229–229; (*b*) I. Haque and J. L. Wood, *J. Mol. Struct.*, 1968, **2**, 217–238.

4 (*a*) L. Turunen and M. Erdélyi, *Chem. Soc. Rev.*, 2020, **49**, 2688–2700; (*b*) S. B. Hakkert and M. Erdélyi, *J. Phys. Org. Chem.*, 2015, **28**, 226–233; (*c*) L. Turunen, U. Warzok, R. Puttreddy, N. K. Beyeh, C. A. Schalley and K. Rissanen, *Angew. Chem., Int. Ed.*, 2016, **55**, 14033–14036; (*d*) L. Turunen, A. Peuronen, S. Forsblom, E. Kalenius, M. Lahtinen and K. Rissanen, *Chem. – Eur. J.*, 2017, **23**, 11714–11718; (*e*) R. Puttreddy, P. Kumar and K. Rissanen, *Chem. – Eur. J.*, 2024, **30**, e202304178.

5 K. Padmanabhan, I. C. Paul and D. Y. Curtin, *Acta Crystallogr., Sect. C: Cryst. Struct. Commun.*, 1990, **46**, 88–92.

6 V. Stilinovic, G. Horvat, T. Hrenar, V. Nemec and D. Cincic, *Chem. – Eur. J.*, 2017, **23**, 5244–5257.

7 I. Nicolas, F. Barrière, O. Jeannin and M. Fourmigué, *Cryst. Growth Des.*, 2016, **16**, 2963–2971.

8 D. Dolenc and M. Modec, *New J. Chem.*, 2009, **33**, 2344–2349.

9 (*a*) O. Makhotkina, J. Lieffrig, O. Jeannin, M. Fourmigué, E. Aubert and E. Espinosa, *Cryst. Growth Des.*, 2015, **15**, 3464–3473; (*b*) E. Aubert, E. Espinosa, I. Nicolas, O. Jeannin and M. Fourmigué, *Faraday Discuss.*, 2017, **203**, 389–406; (*c*) V. V. Syamala, E. Aubert, M. Deutsch, E. Wenger, A. Dhaka, M. Fourmigué, M. Nespolo and E. Espinosa, *Acta Crystallogr., Sect. B: Struct. Sci., Cryst. Eng. Mater.*, 2022, **78**,

436–449; (*d*) E. Aubert, I. Nicolas, O. Jeannin, M. Fourmigué and E. Espinosa, *Cryst. Growth Des.*, 2023, **23**, 7798–7810.

10 (*a*) K. Raatikainen and K. Rissanen, *CrystEngComm*, 2011, **13**, 6972–6977; (*b*) K. Raatikainen and K. Rissanen, *Chem. Sci.*, 2012, **3**, 1235–1239; (*c*) G. Anyfanti, A. Bauzá, L. Gentiluomo, J. Rodrigues, G. Portalone, A. Frontera, K. Rissanen and R. Puttreddy, *Front. Chem.*, 2021, **9**, 623595.

11 (*a*) R. Puttreddy, O. Jurček, S. Bhowmik, T. Mäkelä and K. Rissanen, *Chem. Commun.*, 2016, **52**, 2338–2341; (*b*) R. Puttreddy, J. M. Rautiainen, T. Mäkelä and K. Rissanen, *Angew. Chem., Int. Ed.*, 2019, **58**, 18610–18618; (*c*) R. Puttreddy, J. M. Rautiainen, S. Yu and K. Rissanen, *Angew. Chem., Int. Ed.*, 2023, **62**, e202307372.

12 N. Lucchetti, A. Tkacheva, S. Fantasia and K. Muñiz, *Adv. Synth. Catal.*, 2018, **360**, 3889–3893.

13 S. Yu, K. N. Truong, M. Siepman, A. Siiri, C. Schumacher, J. S. Ward and K. Rissanen, *Cryst. Growth Des.*, 2023, **23**, 662–669.

14 (*a*) K. Mori, M. Kobayashi, T. Itakura and T. Akiyama, *Adv. Synth. Catal.*, 2015, **357**, 35–40; (*b*) V. Pace, G. Vilkauskaite, A. Sackus and W. Holzer, *Org. Biomol. Chem.*, 2013, **11**, 1085–1088.

15 N. Savjani, S. J. Lancaster, S. Bew, D. L. Hughes and M. Bochmann, *Dalton Trans.*, 2011, **40**, 1079–1090.

16 A. Artaryan, A. Mardyukov, K. Kulbitski, I. Avigdori, G. A. Nisnevich, P. R. Schreiner and M. Gandelman, *J. Org. Chem.*, 2017, **82**, 7093–7100.

17 (*a*) P. Politzer, J. S. Murray and T. Clark, *Phys. Chem. Chem. Phys.*, 2010, **12**, 7748–7757; (*b*) T. Clark, M. Hennemann, J. S. Murray and P. Politzer, *J. Mol. Model.*, 2007, **13**, 291–296.

18 (*a*) C. H. Suresh and S. Anila, *Acc. Chem. Res.*, 2023, **56**, 1884–1895; (*b*) E. Aubert, I. Nicolas, O. Jeannin, M. Fourmigué and E. Espinosa, *Cryst. Growth Des.*, 2023, **23**, 7798–7810.

19 A. J. Peloquin, C. D. McMillen and W. T. Pennington, *CrystEngComm*, 2021, **23**, 6098–6106.

20 R. B. Walsh, C. W. Padgett, P. Metrangolo, G. Resnati, T. W. Hanks and W. T. Pennington, *Cryst. Growth Des.*, 2001, **1**, 165–175.

21 J.-L. Syssa-Magale, K. Boubekeur, P. Palvadeau, A. Meerschaut and B. Schollhorn, *CrystEngComm*, 2005, **7**, 302–308.

22 C. Laurence, J. Graton, M. Berthelot and M. J. El Ghomari, *Chem. – Eur. J.*, 2011, **17**, 10431–10444.

23 A. J. Guzmán Santiago, C. A. Brown, R. D. Sommer and E. A. Ison, *Dalton Trans.*, 2020, **49**, 16166–16174.